Journal of the Optical Society of America B
OPTICAL PHYSICS

Improving the visible light communication localization system using Kalman filtering with averaging

Eman Shawky,[1,*] Mohamed El-Shimy,[1] Amr Mokhtar,[1] El-Sayed A. El-Badawy,[1] and Hossam M. H. Shalaby[1,2]

[1]Electrical Engineering Department, Faculty of Engineering, Alexandria University, Alexandria 21544, Egypt
[2]Department of Electronics and Communications Engineering, Egypt-Japan University of Science and Technology (E-JUST), Alexandria 21934, Egypt
*Corresponding author: Eman.shawky@alexu.edu.eg

Received 13 April 2020; revised 15 June 2020; accepted 6 July 2020; posted 7 July 2020 (Doc. ID 395056); published 5 August 2020

Two techniques are proposed for improving the accuracy of localization estimation in indoor visible light communication systems, namely, averaging and Kalman filtering with averaging schemes. In the averaging technique, the receiver position is estimated using the received signal strength (RSS) indication method multiple times (e.g., N samples), and the acquired estimations are averaged over all samples. To further improve the localization, the Kalman filtering algorithm is adopted to estimate the received power over N samples, followed by applying the RSS technique on the average received power. The proposed techniques are analyzed mathematically, considering the effects of both line-of-sight (LOS) and first-reflection from non-LOS propagations. The performance of the proposed techniques is determined by evaluating the positioning errors in a typical room. The results are compared to that of the traditional RSS system. Simulation results reveal that an improvement of about 33.3% in the average positioning error is achievable when using the averaging scheme as compared to that of the traditional RSS scheme. This improvement increases to 72.2% when adopting the proposed Kalman filtering scheme.

https://doi.org/10.1364/JOSAB.395056

1. INTRODUCTION

Visible light communication (VLC) systems will lead to an immense revolution in communications techniques in the next few years [1]. Indeed, they will provide high data transmission rates along with illumination for indoor environments. In addition, they have a high potential for indoor localization compared to RF techniques. Specifically, RF techniques suffer from high interference problems and lack positioning accuracy and coverage [2,3].

Traditional methods of implementing VLC positioning include the time of arrival (TOA) technique, based on the absolute arrival time of optical signals [4], angle of arrival (AOA) technique, based on the intersection of several pairs of angle direction lines [5–7], time difference of arrival (TDOA) technique, based on the difference between the arrival times between signals from at least three transmitters [8], and received signal strength (RSS) technique, based on measuring the attenuation of optical signal strengths emitted by at least three transmitters [5–7,9]. To achieve more accurate localization, a novel solution that provides accurate and high-speed indoor navigation via the designs of an elaborate flicker-free line coding scheme and a lightweight image processing algorithm appears in Ref. [10]. A fusion positioning system based on an extended Kalman filter (KF) is demonstrated in Refs. [11,12]. The KF can fuse inertial navigation and visible light positioning data in order to solve the problem of system failure and decreased accuracy. In Ref. [13], the authors study the tracking of a VLC user when the availability of the VLC access point (AP) link changes over the user's route.

In this paper, we aim at improving the accuracy of localization estimation in indoor VLC systems by proposing two new techniques, namely, averaging and Kalman filtering schemes. In the averaging technique, the receiver position is estimated using the RSS indication method multiple times (e.g., N samples), and the acquired estimations are averaged over all samples. For further improving the localization, the Kalman filtering algorithm is adopted to estimate the received power over N samples, followed by applying the RSS technique on the average received power. Tracking mobile users with a KF can increase the accuracy of the positioning, but the generic KF does not consider instant changes in the measurement method. In order to include this information in the position estimation, we implement an adaptive KF by modifying the filter parameters based on the availability of APs to the user. The proposed techniques

are analyzed mathematically, considering the effects of both line-of-sight (LOS) and first-reflection from non-LOS (NLOS) propagations. The performance of the proposed techniques is determined by evaluating the positioning errors in a typical room. The results are compared to those of the traditional RSS system.

The remainder of this paper is organized as follows. Section 2 presents the channel modeling of a VLC system. Section 3 demonstrates the methodology of localization using the proposed averaging technique. The KF technique and its algorithm are explained in Section 4. Simulation results and discussion are presented in Section 5. Finally, concluding remarks are given in Section 6.

2. INDOOR VLC LINK MODEL

Figure 1 shows the indoor optical wireless channel model for both LOS and NLOS propagations. We assume that we have four ceiling light-emitting diode (LED) transmitters, located at $T_{X,i} = (x_i, y_i, z_i)$, $i \in \{1, 2, 3, 4\}$, and one photodetector, located at $R_X = (x_0, y_0, z_0)$.

A. LOS Link

The gain of the LOS optical link from the ith LED, $i \in \{1, 2, 3, 4\}$, to the photodetector can be modeled as [14]

$$H^i_{\text{LOS}} = \frac{m+1}{2\pi d_i^2}\cos^m(\phi_i) A_R \cos(\psi_i)\, T_s(\psi_i) g(\psi_i), \quad (1)$$

where m is the Lambertian order, d_i is the distance between transmitter i and the receiver, ϕ_i is the irradiance angle, ψ_i is the incidence angle, $T_s(\cdot)$ and $g(\cdot)$ are the gains of the optical filter and concentrator at the receiver (assumed here as unity gain), respectively, and A_R is the detector effective area.

B. NLOS Link

For a one-path indoor NLOS channel with the reflection point located at $p = (x, y, z)$, as shown in Fig. 1, the gain of first-reflection H^{ip}_{NLOS} from transmitter i is given by [14]

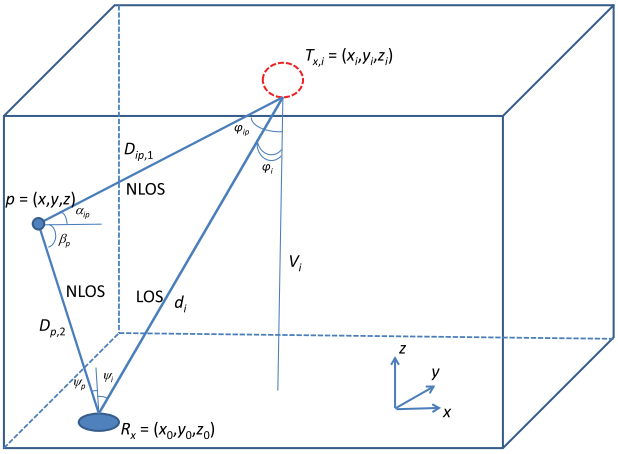

Fig. 1. LOS/NLOS channel model for indoor applications.

$$H^{ip}_{\text{NLOS}} = \frac{m+1}{2\pi D^2_{ip,1} D^2_{p,2}}\cos^m(\phi_{ip}) \cos(\alpha_{ip}) \cdot dA_p \times \rho \cos(\beta_p) \cos(\psi_p)\, T_s(\psi_p) g(\psi_p) A_R, \quad (2)$$

where $D_{ip,1}$ is the distance between transmitter i and reflection point p, $D_{p,2}$ is the distance between reflection point p and receiver R_X, ϕ_{ip} and ψ_p are the NLOS irradiance and incidence angles with respect to point p, respectively, α_{ip} and β_p are the incidence and irradiance angles at the reflection point on the wall, respectively, ρ is the wall reflectivity (assumed to be $\rho = 0.8$), and dA_p represents the area of the reflection point on the wall.

The total NLOS channel gain for ith transmitter H^i_{NLOS} is given by collecting the reflections from the four walls [15]:

$$H^i_{\text{NLOS}} = \sum_{j=1}^{4} H^i_{\text{NLOS,wall}\,j}, \quad (3)$$

where $H^i_{\text{NLOS,wall}\,j}$ is the collection of reflections from transmitter i to wall j, and can be obtained by integrating Eq. (2) over (x, z) or (y, z) based on the wall location, such that

$$H^i_{\text{NLOS,wall}\,j} = \iint_{(x,z)\text{ or }(y,z)} \frac{m+1}{2\pi D^2_{ip,1} D^2_{p,2}}\cos^m(\phi_{ip}) \cos(\alpha_{ip})\rho \times \cos(\beta_p) \cos(\psi_p)\, T_s(\psi_p) g(\psi_p) A_R \mathrm{d}A_p. \quad (4)$$

1. Parameters' Relations

The parameters of Eq. (4) can be determined as follows:

$$D_{ip,1} = \sqrt{(T_{X,i} - p)(T_{X,i} - p)^T},$$
$$D_{p,2} = \sqrt{(p - R_X)(p - R_X)^T}, \quad (5)$$

where a^T is the transpose operator for row vector a. From Fig. 1 and by using triangle calculations, the angles ϕ_{ip}, α_{ip}, ψ_p, and β_p can be found as follows:

$$\cos(\phi_{ip}) = \frac{|z_i - z|}{D_{ip,1}}, \quad \alpha_{ip} = \frac{\pi}{2} - \phi_{ip},$$
$$\cos(\psi_p) = \frac{|z - z_0|}{D_{p,2}}, \quad \beta_p = \frac{\pi}{2} - \psi_p. \quad (6)$$

3. PROPOSED LOCALIZATION METHODOLOGY USING AN AVERAGING RSS TECHNIQUE

To get the receiver location, the traditional trilateration localization technique is employed using the RSS from three LED transmitters having the maximum received levels [16]. Our approach here is to average the estimated receiver position over a certain number of measurements in order to reduce the localization error. This reduction in error comes at the cost of increasing the system's mathematical complexity. Figure 2 shows a simple block diagram that demonstrates this approach.

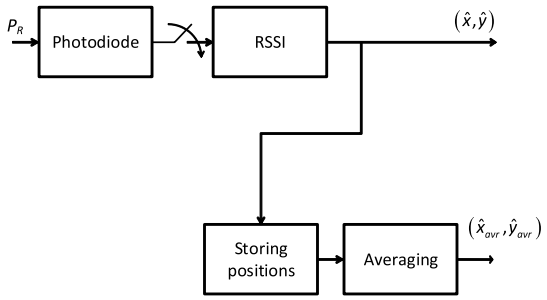

Fig. 2. Block diagram of proposed averaging positioning scheme.

A. Received Signal Strength Technique

Using Eq. (1), the received LOS power from transmitter $i \in \{1, 2, 3, 4\}$ can be written as

$$P_{R,i} = \left(\frac{m+1}{2\pi d_i^2}\cos^{m+1}(\phi_i) A_R\right) P_{T,i}, \tag{7}$$

where $P_{T,i}$ is the transmitted power of ith LED. Here, we assume that $\psi_i = \phi_i$, which is determined from Fig. 1 as

$$\cos(\phi_i) = \frac{V}{d_i}, \tag{8}$$

where V is the vertical distance between the transmitter and receiver, assumed constant. Accordingly, the distance between transmitter i and the receiver can be evaluated as

$$d_i = \sqrt[m+3]{\frac{(m+1)V^{m+1}A_R P_{T,i}}{2\pi P_{R,i}}}. \tag{9}$$

If we consider the effect of NLOS as well, the total power collected at the receiver is obtained by modifying Eq. (7) to

$$P_{R,i} = (H^i_{\text{LOS}} + H^i_{\text{NLOS}}) P_{T,i}. \tag{10}$$

B. Linear Least-Square Method

To estimate the receiver location, the linear least-square (LLS) estimation is commonly used. Let (x_i, y_i), $i \in \{1, 2, 3\}$, be the horizontal coordinates of transmitter i and $d_{L,i}$ be the horizontal distance of the receiver from transmitter i. The range equation can be written in the form

$$(\hat{x} - x_i)^2 + (\hat{y} - y_i)^2 = d^2_{L,i}, \quad i \in \{1, 2, 3\}, \tag{11}$$

where $(\hat{x}, \hat{y})$ is the estimated horizontal location of the receiver. The last system of equations can be written in matrix form as

$$A\hat{X} = B, \tag{12}$$

where

$$\hat{X} = [\,\hat{x}\ \hat{y}\,]^T,$$

$$A = \begin{bmatrix} x_2 - x_1 & y_2 - y_1 \\ x_3 - x_1 & y_3 - y_1 \end{bmatrix},$$

$$B = [\,b_{21}\ b_{31}\,]^T. \tag{13}$$

Here, for any $m \in \{2, 3\}$,

$$b_{m1} = (\hat{x} - x_1)(x_m - x_1) + (\hat{y} - y_1)(y_m - y_1). \tag{14}$$

The solution to Eq. (12) is

$$\hat{X} = (A^T A)^{-1} A^T B. \tag{15}$$

C. Complexity Analysis

The complexity of the proposed averaging RSS technique can be analyzed by counting the number of mathematical operations required to solve the LLS method once and then multiplying the result by the number of samples. The LLS method is done for each sample to estimate the position of the receiver. Specifically, each operation (addition, subtraction, multiplication, division) can be configured as one floating-point operation (flop). Accordingly, we get 39 flops for the LLS method. Multiplying the number of flops by the number of samples and adding one flop for the average operation, we get a total number of $39N + 1$ flops for proposed system, where N is the number of samples. That is, the complexity increases linearly with the number of samples.

To determine the complexity of Kalman filtering with the averaging localization method, we notice that here we get estimates of received powers for the samples one time then average the received powers. These operations do not depend on the number of samples. Thus, the total number of flops is constant even for an increased number of samples. We conclude that the complexity of the proposed averaging RSS is more than that of Kalman filtering with averaging.

4. PROPOSED LOCALIZATION METHODOLOGY USING KALMAN FILTERING WITH AVERAGING

The KF is considered an efficient recursive filter. It estimates the internal state of a linear system from a series of noisy measurements then produces estimates of unknown variables that tend to be more accurate than those based on a single measurement.

In this section, a KF algorithm is used to further improve the estimation of the receiver position. First, the KF estimates several samples of measured received powers. Next, the average of these estimated power values is calculated. Using this estimated average power, the position of the receiver can be found by the RSS technique. The block diagram of the proposed Kalman filtering with averaging technique is shown in Fig. 3. The flowchart in Fig. 4 shows the steps of using a KF with the AVG method, which explains the algorithm flow. The KF algorithm recursively estimates the state of variables in the system in two phases: prediction and measurement [17,18].

A. Prediction Step

We denote our state vector by x. This state vector represents the measured received power and number of samples used in the process. Based on the estimate at iteration $k-1$, we have state $x_{k-1|k-1}$. The next step k of the system dynamics $x_{k|k-1}$ is evaluated as

$$x_{k|k-1} = F_k x_{k-1|k-1} + v_k, \tag{16}$$

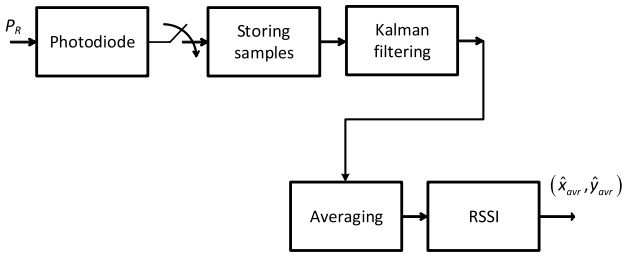

Fig. 3. Block diagram of proposed Kalman filtering algorithm.

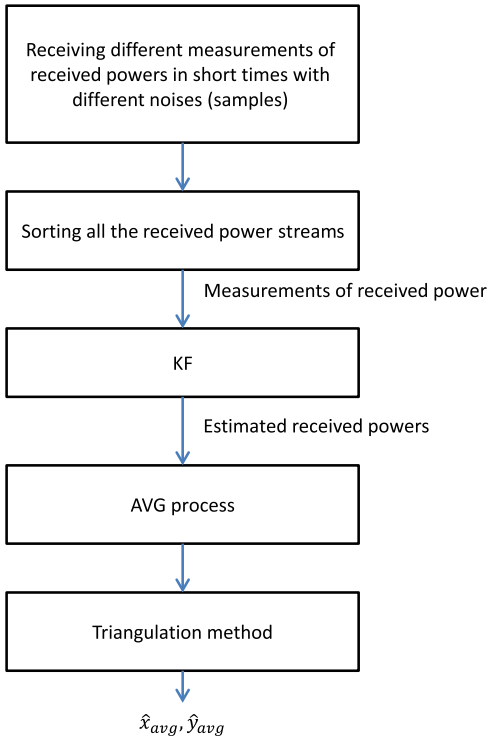

Fig. 4. Flowchart of proposed Kalman filtering algorithm.

where F_k is the state transition matrix, and v_k is a white process noise. The corresponding state covariance matrix is given by

$$P_{k|k-1} = F_k P_{k-1|k-1} F_k^T + Q_k, \tag{17}$$

where Q_k is the covariance of the noise process.

B. Measurement Step

The updated state variable $x_{k|k}$ and updated state covariance matrix $P_{k|k}$ are given by

$$x_{k|k} = x_{k|k-1} + K_k y_k,$$
$$P_{k|k} = (I - K_k H_k) P_{k|k-1}, \tag{18}$$

respectively, where K_k is the Kalman gain, y_k is the error vector, and H_k is the observation model:

$$K_k = P_{k|k-1} H_k^T S_k^{-1},$$
$$y_k = z_k - H_k x_{k|k-1}. \tag{19}$$

Here, z_k denotes the measurement vector:

$$z_k = H_k x_k + w_k, \tag{20}$$

where w_k is the measurement noise. Also, S_k is the innovation matrix, which relates the covariance of state variables to the measurement vector:

$$S_k = H_k P_{k|k-1} H_k^T + R_k, \tag{21}$$

where R_k is the covariance of measurement noise.

5. SIMULATION AND DISCUSSION

In this section, simulation results for the proposed system are presented and compared with those of traditional systems. The main parameters used in the simulations for the VLC link are listed in Table 1.

A. Positioning Error

In our simulation, the performance measure is determined by the positioning error:

$$\mathcal{E}_{\text{position}} = \sqrt{(\hat{x} - x_0)^2 + (\hat{y} - y_0)^2}, \tag{22}$$

where (x_0, y_0) is the receiver's horizontal location, and $(\hat{x}, \hat{y})$ is its estimated location. Figure 5 shows the average error in receiver positioning for different numbers of samples. The positioning error performance for each sample is related to average the storing positions stream (X_{avg}, Y_{avg}) and where each sample has different noise that get a jitter of positioning error performance.

It is clear that the error can be reduced to less than 10% of its maximum value by averaging over 50 samples.

The mathematics behind this is that for any number of samples n, the expected value of the positioning error is

$$E\{\mathcal{E}_{\text{position}}(n)\} = 0. \tag{23}$$

For ergodic processes, we have

$$\lim_{N\to\infty} \frac{\sum_{n=1}^{N} \mathcal{E}_{\text{position}}(n)}{N} = E\{\mathcal{E}_{\text{position}}(n)\} = 0, \tag{24}$$

where N is the total number of samples. Accordingly, $\sum_{n=1}^{N} \mathcal{E}_{\text{position}}(n)/N$ is a decreasing function with N.

Table 1. Simulation Parameters

Parameter	Value
Room dimensions	$5 \times 5 \times 3$ m^3
Number of transmitters	4
Total transmitted power per T_x	30 W
Locations of LEDs	(1.25, 1.25, 3), (1.25, 3.75, 3), (3.75, 1.25, 3), (3.75, 3.75, 3) m
FOV of photodetector	70°
Signal-to-noise ratio (SNR)	20
Active area of photodetector	1 cm^2
Wall reflectivity ρ	0.8
Number of samples	50
Range of receiver in room	(1–3.5) m over both x, y axes

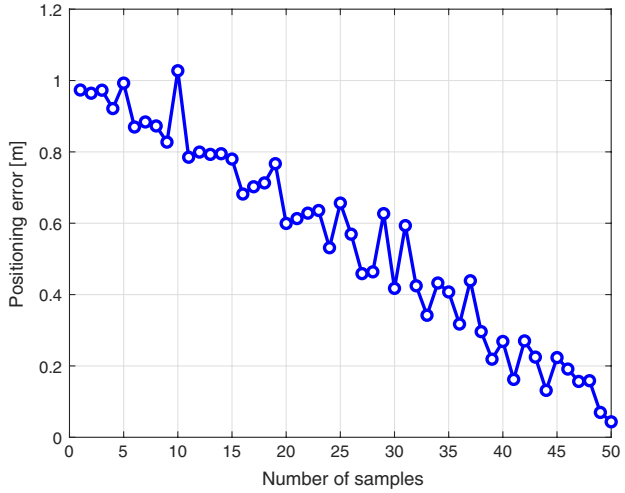

Fig. 5. Comparison between average positioning errors versus number of samples in averaging RSS technique.

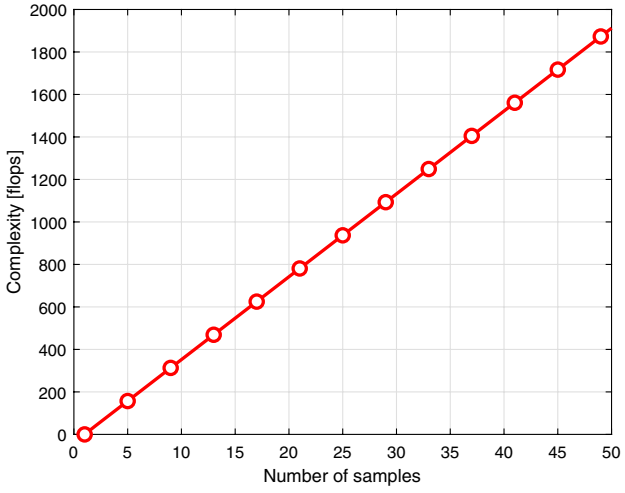

Fig. 6. Complexity of the averaging RSS method.

This reduction, however, comes at the cost of increasing the mathematical complexity of the system, as shown in Fig. 6. The complexity is calculated according to the number of operations, which increases as the number of samples increases.

B. Averaging RSS and Traditional RSS Techniques

The RSS variations of the positioning error at every sample is shown in Fig. 7(a) for receiver position $(x_0, y_0) = (1, 1)$, considering the effect of LOS only. At the place [1,1], $(X_{\text{avg}}, Y_{\text{avg}}) = (0.7234, 0.7662)$ for 50 samples with error in the accuracy nearly (0.2766,0.2338).

For the RSS method, there are random deviations between the estimates and real values, which are caused due to system noises. The average of this random noise is clearly zero. Accordingly, the proposed averaging RSS can cope with it.

The positioning error using the proposed averaging RSS technique (with 100 samples) is plotted in the same figure as well. The improvement using the proposed technique is clear

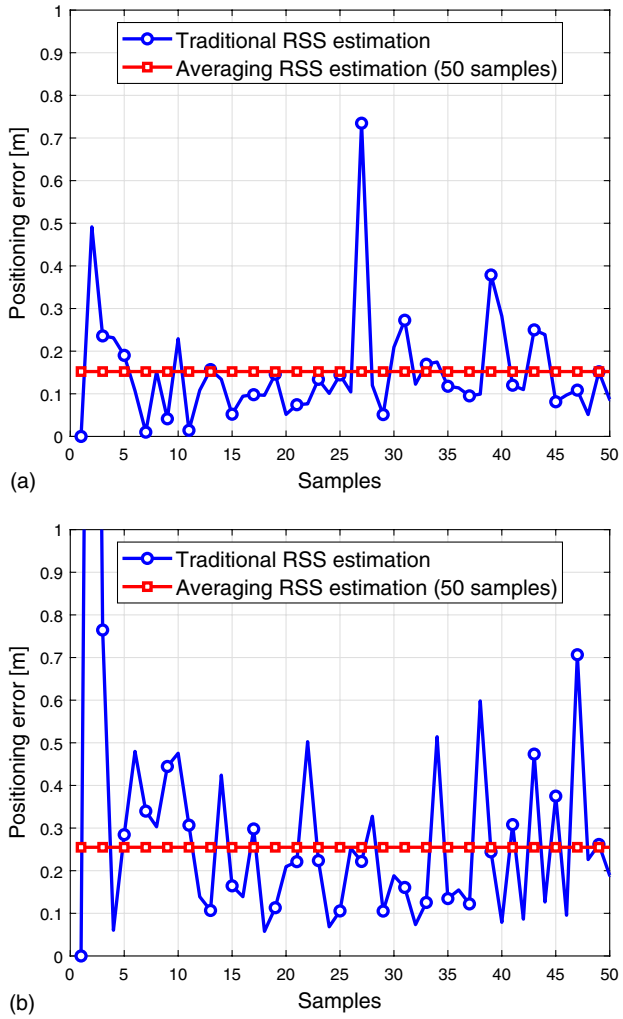

Fig. 7. Positioning error for both traditional RSS and averaging RSS techniques at position (1, 1), considering the effects of (a) LOS only and (b) both LOS and NLOS.

in the figure. Indeed, traditional RSS errors can reach more than 0.6 m (42.4%), while the error when using the proposed averaging RSS is only 0.217 m (15.3%), i.e., an improvement of about 27.1% is achievable when using the proposed scheme. The effects of both LOS and NLOS are studied for receiver position $(x_0, y_0) = (1, 1)$ as well, and the results are plotted in Fig. 7(b). The effect of both LOS and NLOS on averaging RSS tracks' estimations for the x axis is shown in Fig. 8. Traditional RSS errors can reach more than 0.7 m (49.5%), while the error when using the proposed averaging RSS is only 0.255 m (18%), i.e., an improvement of about 31.5% is achievable when using the proposed scheme.

C. Kalman Filtering, Averaging RSS, and Traditional RSS Techniques

In this subsection, we demonstrate several comparisons between the performance of three methods: traditional RSS, proposed averaging RSS, and proposed Kalman filtering with averaging. We use the same parameters as given for the VLC link in Table 1.

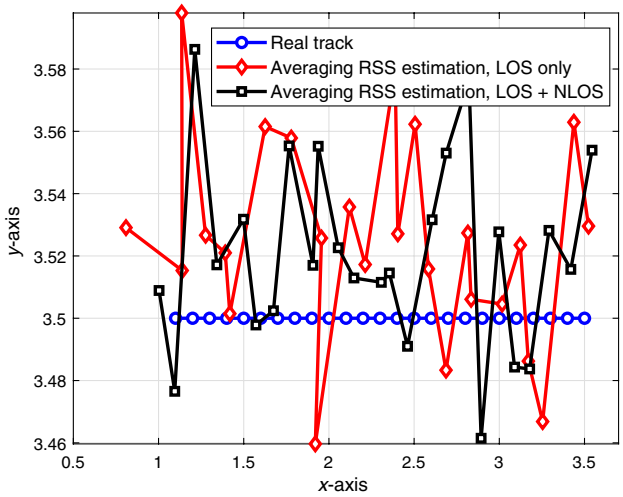

Fig. 8. Comparison between LOS and NLOS effects for averaging RSS method.

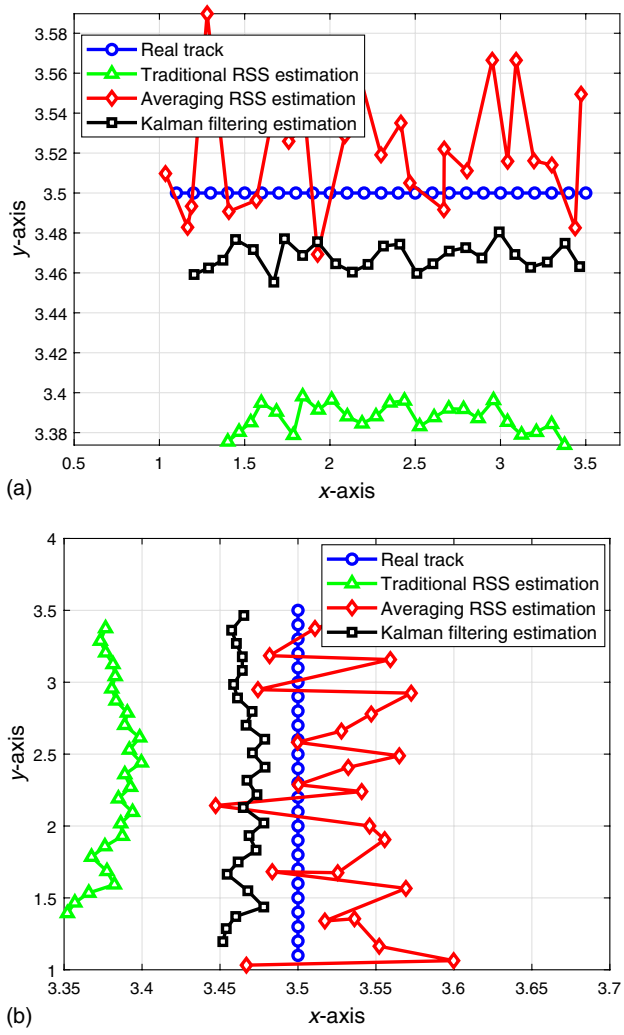

Fig. 9. Track estimations using traditional and proposed techniques for (a) an x path and (b) a y path, for LOS propagation.

1. LOS Propagation

The effects of LOS on only two tracks' estimations for both x and y paths are presented in Figs. 9(a) and 9(b) for both x and y paths, respectively.

In addition, Figs. 10(a) and 10(b) show similar results for square and circular tracks, respectively.

It is clear in the figures that both tracks' estimations are closer to the real one when using the proposed techniques. Furthermore, the figures indicate that adopting KF estimation further reduces the positioning error and provides an estimate that is very close to reality. The average errors in detecting the position of the receiver are summarized in Table 2 for the three techniques. Specifically, the average errors when using traditional RSS, proposed averaging RSS, and proposed Kalman filtering with averaging are 18 cm, 12 cm, and 5 cm, respectively. That is, the improvement in estimation accuracy when using the proposed averaging RSS and Kalman filtering with averaging are 33.3% and 72.2%, respectively.

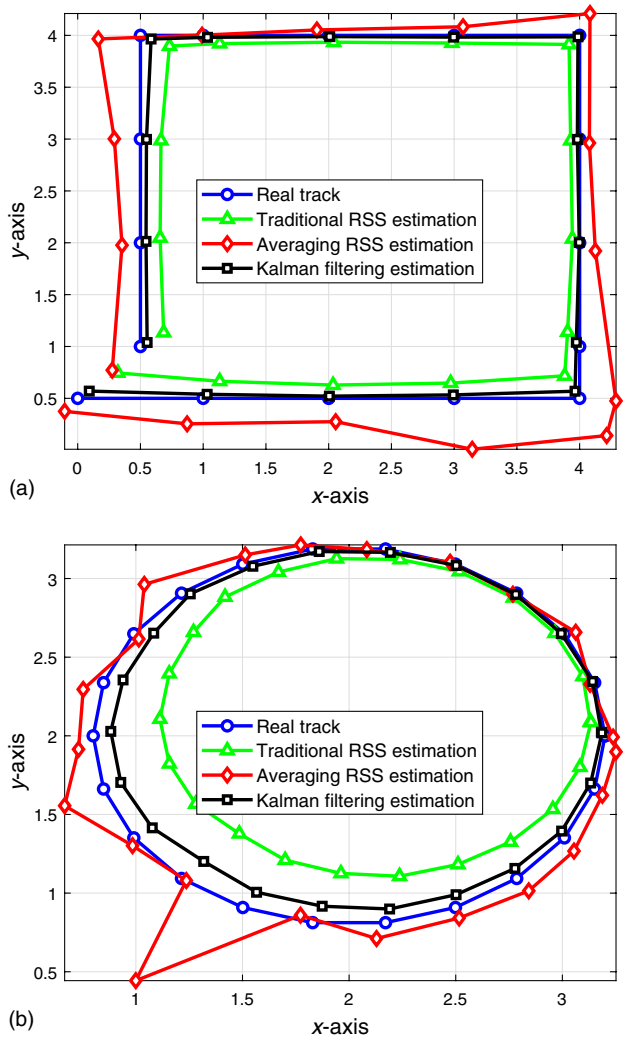

Fig. 10. Track estimations using traditional and proposed techniques for (a) a square track and (b) a circular track, for LOS propagation.

Table 2. Accuracy for Different Techniques Related to Traditional RSS

Localization Method	Average Positioning Error	Percentage Improvement
Traditional RSS	18 cm	–
Averaging RSS	12 cm	33.3%
Kalman filtering	5 cm	72.2%

2. Both LOS and NLOS Propagations

The effects of both LOS and NLOS on two tracks' estimations for both x and y paths are presented in Figs. 11(a) and 11(b) for both x and y paths, respectively.

In addition, Fig. 12 shows the results for a square track for both LOS and NLOS propagations.

It is clear in the figure that both tracks' estimations are closer to the real one when using the LOS effect only rather than using the effects of both LOS and NLOS. The gain results from NLOS being considered unwanted signal noise, and adding it decreases accuracy. These simulations have been done in a typical room as shown in Table 1. Specifically, the figures show

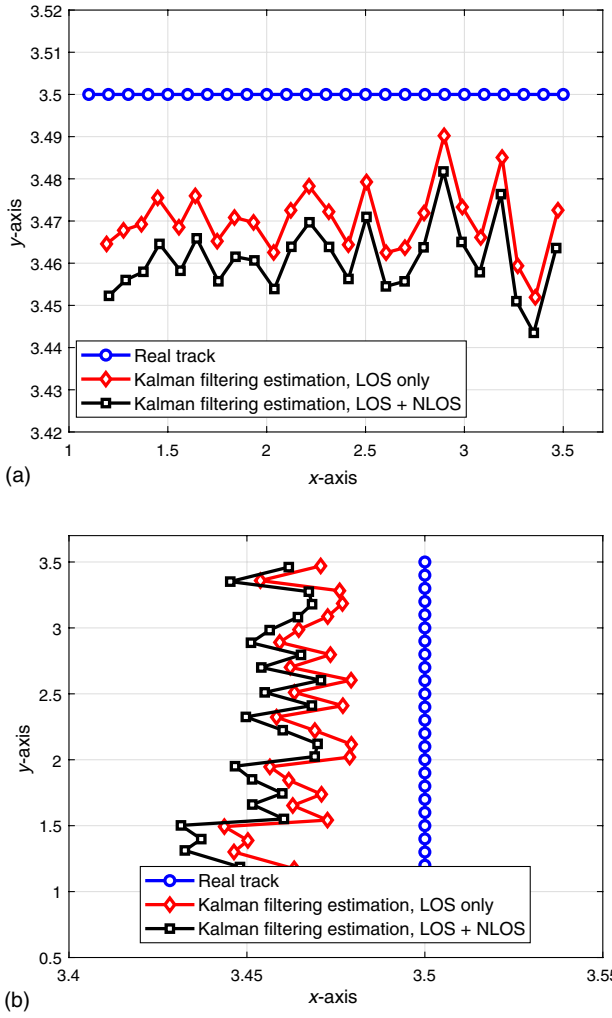

Fig. 11. Comparison between Kalman filtering track estimation for both LOS and NLOS propagations for (a) an x path and (b) a y path.

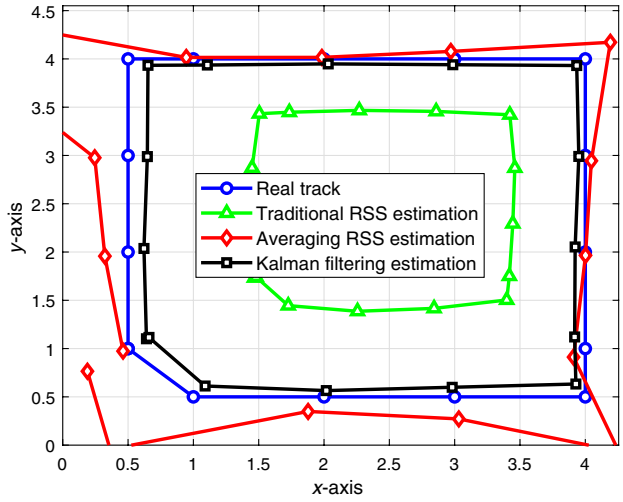

Fig. 12. Comparison between Kalman filtering square track estimation for both LOS and NLOS propagations.

the proposed Kalman filtering with averaging only because this method outperforms other methods in previous figures.

3. Kalman Filtering Response

The Kalman filtering response for a random position estimation is presented in Fig. 13. The filter input is a measured value of received power, while the filter output is the corresponding estimated value at different numbers of samples, where NLOS here is considered. It is clear in figure that the filtering response (estimated value) is very close to the real value when the number of samples is greater than 11 samples only.

D. Mean Squared Error Method

In this section, we adopt the mean squared error (MSE) method to evaluate the performance of our proposed positioning algorithms. Suppose that we estimate a position location using N samples with a population of calculated coordinates: $\{(x_1, y_1), (x_2, y_2), \ldots, (x_N, y_N)\}$. The MSE is given by [19]

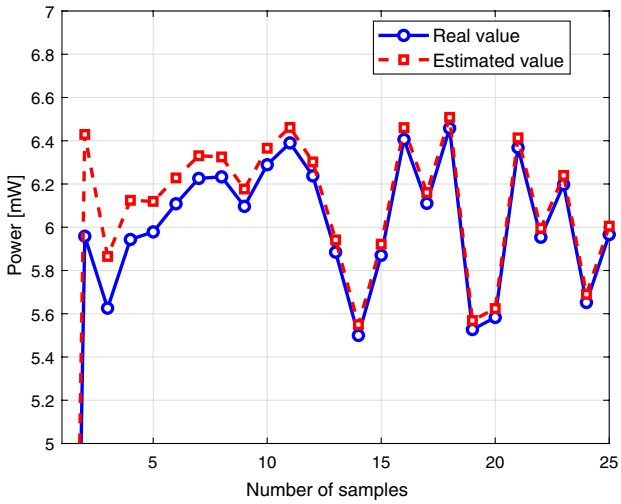

Fig. 13. Response of Kalman filtering technique.

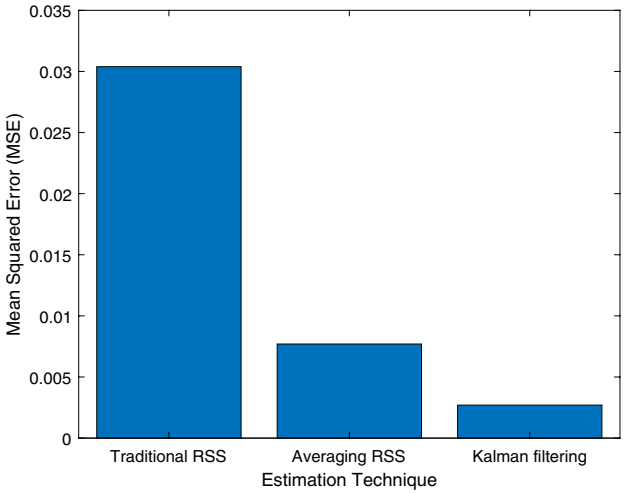

Fig. 14. Mean squared errors for different estimation techniques.

$$\mathrm{MSE} = \frac{1}{N}\sum_{i=1}^{N}\left[(x_i - \bar{x})^2 + (y_i - \bar{y})^2\right], \tag{25}$$

where $(\bar{x}, \bar{y})$ is the mean of the calculated coordinate:

$$\bar{x} = \frac{1}{N}\sum_{i=1}^{N} x_i, \quad \bar{y} = \frac{1}{N}\sum_{i=1}^{N} y_i. \tag{26}$$

In Fig. 14, we plot the MSE for the three estimation techniques used in the paper. We use 50 samples in our simulation with the same parameters as those listed in Table 1. It is clear that the proposed system using a KF has the least MSE.

E. Cumulative Distribution Function

The cumulative distribution function (CDF) is another way to compare the different estimation techniques. We plot in Fig. 15 the CDFs for the three estimation techniques used in paper. Again, the proposed Kalman filtering method shows the least values for CDFs when compared to both traditional and averaging RSS techniques.

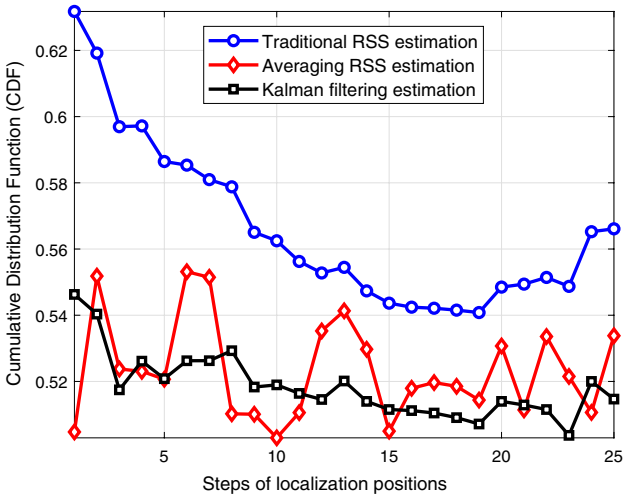

Fig. 15. Cumulative distribution functions for different estimation techniques.

F. Position Estimation Accuracy Comparison

As mentioned in the Introduction, several techniques have been proposed for indoor localization based on VLC technology. In this section, we provide a comparison between our position estimation accuracy and that of previous works for the same simulation parameters. The results of this comparison are summarized in Table 3.

In Ref. [3], an analytical model is developed considering both LOS and NLOS effects with FOV = 80°, transmitted power of 10 W, detector effective area $A_R = 0.5\ \mathrm{cm}^2$, and room dimensions of (5, 5, 3) m. They achieve an accuracy of 5 cm. The corresponding accuracies achieved for both the proposed averaging RSS and Kalman filtering are 3.7 cm and 3.1 cm, respectively.

In Ref. [5], a two-phase hybrid algorithm for estimating the location of a mobile node, which has the capability of measuring signal strength, azimuth, and elevation, in a smart space environment over the visible light channel is proposed. For the system parameters in Ref. [5], with the effects of both LOS and NLOS, FOV = 10 − 180°, transmitted power is 1.9 W, $A_R = 0.81\ \mathrm{cm}^2$, room dimensions are (4, 4, 3.5) m, and wall reflectivity is 60%; the achieved accuracy is 13.95 cm. The corresponding accuracies achieved for both proposed averaging RSS and Kalman filtering are 9.1 cm and 4.8 cm, respectively.

The effect of only LOS is considered in Ref. [7], where the hybrid utilization of AOA and RSS information in VLC systems is investigated for 3D localization with FOV = 85°, transmitted power of 1 W, $A_R = 0.81\ \mathrm{cm}^2$, and room dimensions of (5, 4, 3) m. The achieved accuracy is 10 cm, while the corresponding accuracies achieved for both proposed averaging RSS and Kalman filtering are 6.17 cm and 1.75 cm, respectively.

In Ref. [12], a fusion positioning system based on extended KFs is proposed, which can fuse the VLC position and the inertial navigation data. The parameters are a room with dimensions of (3.6, 3.26, 2.5) m, $A_R = 1\ \mathrm{cm}^2$, transmitted power of 17 W, and seven LEDs; the achieved accuracy is 14.5 cm. The corresponding accuracies achieved for both proposed averaging RSS and Kalman filtering are 17.4 cm and 3.5 cm, respectively.

In Ref. [13], the authors study tracking a VLC user when the availability of the VLC AP link changes over the user's route. They use room dimensions of (6, 6, 3) m with seven LEDs, FOV = 25°, and $A_R = 1\ \mathrm{cm}^2$. The obtained accuracy is 5 cm, while the corresponding accuracies achieved for both proposed averaging RSS and Kalman filtering are 11 cm and 2.3 cm, respectively.

It is clear from the discussion above and Table 3 that both the proposed averaging RSS and Kalman filtering with averaging techniques achieve better accuracy than those proposed in Refs. [3,5,7]. Since the authors in Refs. [12,13] adopt Kalman filtering, they have better accuracy than our proposed averaging method. However, employing Kalman filtering with averaging gives better accuracy.

Table 3. Position Estimation Accuracy Comparison

References	System Parameters	Reference Accuracy	Averaging System Accuracy	Kalman Filtering Accuracy
[3]	LOS, FOV = 80°, $P_T = 10$ W, $A_R = 0.5$ cm^2, (5, 5, 3) m^3, RSS	5 cm	3.7 cm	3.1 cm
[5]	LOS/NLOS, FOV = 10−180°, $P_T = 1.9$ W, $A_R = 0.81$ cm^2,	13.95 cm	9.1 cm	4.8 cm
[7]	LOS, FOV = 85°, $P_T = 1$ W, $A_R = 0.81$ cm^2, (5, 4, 3) m^3, (AOA, RSS)	10 cm	6.17 cm	1.75 cm
[12]	LOS, FOV = 80°, $P_T = 17$ W, $A_R = 1$ cm^2, (3.6, 3.26, 2.5) m^3, EKF	14.5 cm	17.4 cm	3.5 cm
[13]	LOS, FOV = 25°, $P_T = 17$ W, $A_R = 1$ cm^2, (6, 6, 3) m^3, EKF	5 cm	11 cm	2.3 cm

6. CONCLUDING REMARKS

Two techniques have been proposed for improving the accuracy of localization estimation in indoor VLC systems, namely, averaging and Kalman filtering with averaging schemes. Specifically, in the averaging technique, the receiver position is determined by averaging multiple samples of RSS estimations. In the Kalman filtering with averaging algorithm, the position is determined by an RSS estimation of a Kalman filtering averaged multiple received power samples. The proposed techniques have been analyzed mathematically, taking into account the effects of both LOS and first-reflection from NLOS propagations. The positioning estimation accuracy of the proposed techniques have been evaluated in a typical room, and the results are compared to those of traditional RSS systems. Simulation results reveal that an improvement of about 33.3% in estimation accuracy is achievable when using the averaging scheme as compared to that of the traditional RSS scheme. This improvement increases to 72.2% when adopting the proposed Kalman filtering with averaging scheme.

Disclosures. The authors declare that there are no conflicts of interest related to this paper.

REFERENCES

1. H. Naveed, N. Aqsa, P. M. Adeel, J. Tariq, and Y. Chau, "Indoor positioning using visible LED lights: a survey," ACM Comput. Surv. **48**, 1–20 (2015).
2. L. E. M. Matheus, A. B. Vieira, L. F. M. Vieira, M. A. M. Vieira, and O. Gnawali, "Visible light communication: concepts, applications and challenges," Commun. Surveys Tutorials **21**, 3204–3237 (2019).
3. F. Mousa, N. Almaadeed, K. Busawon, A. Bouridane, R. Binns, and I. Elliot, "Indoor visible light communication localization system utilizing received signal strength indication technique and trilateration method," Opt. Eng. **57**, 016107 (2018).
4. T. Q. Wang, Y. A. Sekercioglu, A. Neild, and J. Armstrong, "Position accuracy of time-of-arrival based ranging using visible light with application in indoor localization systems," J. Lightwave Technol. **31**, 3302–3308 (2013).
5. M. S. Islam and R. Klukas, "Indoor positioning through integration of optical angles of arrival with an inertial measurement unit," in *IEEE/ION Position, Location and Navigation Symposium* (2012), pp. 408–413.
6. S. Yang, H. Kim, Y. Son, and S. Han, "Three-dimensional visible light indoor localization using AOA and RSS with multiple optical receivers," J. Lightwave Technol. **32**, 2480–2485 (2014).
7. A. Şahin, Y. S. Eroğlu, I. Güvenç, N. Pala, and M. Yüksel, "Hybrid 3-D localization for visible light communication systems," J. Lightwave Technol. **33**, 4589–4599 (2015).
8. S. Jung, S. Hann, and C. Park, "TDOA-based optical wireless indoor localization using LED ceiling lamps," IEEE Trans. Consum. Electron. **57**, 1592–1597 (2011).
9. H. Kim, D. Kim, S. Yang, Y. Son, and S. Han, "An indoor visible light communication positioning system using a RF carrier allocation technique," J. Lightwave Technol. **31**, 134–144 (2013).
10. J. Fang, Z. Yang, S. Long, Z. Wu, X. Zhao, F. Liang, Z. L. Jiang, and Z. Chen, "High-speed indoor navigation system based on visible light and mobile phone," IEEE Photon. J. **9**, 1–11 (2017).
11. Z. Vatansever and M. Brandt-Pearce, "Visible light positioning with diffusing lamps using an extended Kalman filter," in *IEEE Wireless Communications and Networking Conference (WCNC)* (2017), pp. 1–6.
12. A. Y. Z. Li and L. Feng, "Fusion based on visible light positioning and inertial navigation using extended Kalman filters," Sensors **17**, 1093 (2017).
13. Y. S. Eroglu, F. Erden, and I. Guvenc, "Adaptive Kalman tracking for indoor visible light positioning," in *IEEE Military Communications Conference (MILCOM)* (2019), pp. 331–336.
14. Z. Ghassemlooy, W. Popoola, and S. Rajbhandari, *Optical Wireless Communications: System and Channel Modelling with MATLAB* (CRC Press, 2013).
15. C. Huang and X. Zhang, "LOS-NLOS identification algorithm for indoor visible light positioning system," in *20th International Symposium on Wireless Personal Multimedia Communications (WPMC)* (2017), pp. 575–578.
16. M. Shchekotov, "Indoor localization method based on Wi-Fi trilateration technique," in *16th Conference of Fruct Association, ACP* (2014), pp. 177–179.
17. G. Welch and G. Bishop, "An introduction to the Kalman filter," Technical Report 95-041 (University of North Carolina, 2006).
18. Y. Teruyama and T. Watanabe, "Effectiveness of variable-gain Kalman filter based on angle error calculated from acceleration signals in lower limb angle measurement with inertial sensors," Comput. Math. Methods Med. **10**, 398042 (2013).
19. E. C. L. Chan and G. Baciu, *Introduction to Wireless Localization* (Wiley, 2012).